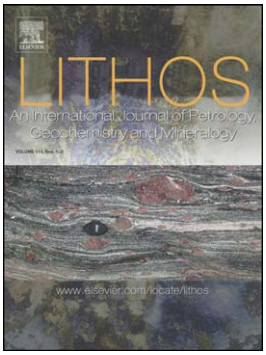

A Toba-scale eruption in the Early Miocene: The Semilir eruption, East Java, Indonesia

Helen R. Smyth, Quentin G. Crowley, Robert Hall, Peter D. Kinny, P. Joseph Hamilton, Daniela N. Schmidt

PII: S0024-4937(11)00205-2
DOI: doi: 10.1016/j.lithos.2011.07.010
Reference: LITHOS 2484

To appear in: *LITHOS*

Received date: 28 March 2011
Revised date: 19 July 2011
Accepted date: 19 July 2011

Please cite this article as: Smyth, Helen R., Crowley, Quentin G., Hall, Robert, Kinny, Peter D., Hamilton, P. Joseph, Schmidt, Daniela N., A Toba-scale eruption in the Early Miocene: The Semilir eruption, East Java, Indonesia, *LITHOS* (2011), doi: 10.1016/j.lithos.2011.07.010

A Toba-scale eruption in the Early Miocene: The Semilir eruption, East Java, Indonesia

Helen R. Smyth [a,b*], Quentin G. Crowley [c, d], Robert Hall [b], Peter D. Kinny [e], P. Joseph Hamilton [e] and Daniela N. Schmidt [f]

[a] CASP, Department of Earth Sciences, University of Cambridge, West Building, 181a Huntingdon Road, Cambridge, CB3 0DH, UK (present address) email: helen.smyth@casp.cam.ac.uk, tel: +44 1223 760700 fax: +44 1223 760701

[b]SE Asia Research Group, Department of Earth Sciences, Royal Holloway University of London, Egham, Surrey, TW20 0EX, UK robert.hall@es.rhul.ac.uk

[c] NERC Isotope Geosciences Laboratory, British Geological Survey, Kingsley Dunham Centre, Keyworth, Nottingham, NG12 5GG, UK

[d] Geology,School of Natural Sciences, Trinity College, Dublin 2, Ireland crowleyq@tcd.ie (present address)

[e] The Institute for Geoscience Research, Department of Applied Geology, Curtin University, Perth 6845, Australia P.Kinny@curtin.edu.au, Joseph.Hamilton@alsglobal.com

[f] Department of Earth Sciences, University of Bristol BS8 1RJ, UK

d.schmidt@bristol.ac.uk

*Corresponding author

Email: helen.smyth@casp.cam.ac.uk Tel: +44 (0)1223 760700 Fax: +44(0)1223 760701

Abstract

The Indonesian archipelago is well known for volcanic activity and has been the location of three catastrophic eruptions in the last million years: Krakatau, Tambora and Toba. However, there are no reports of large magnitude eruptions during the earlier Cenozoic despite a long volcanic record in Indonesia during subduction of Indian Ocean lithosphere since the Eocene. Here we report an Early Miocene major eruption, the Semilir eruption, in south Java, the main phase of which occurred at 20.7 ± 0.02 Ma. This major volcanic eruption appears similar in scale, but not in type, to the 74 ka Toba event. Its products can be identified elsewhere in Java and are likely to have been distributed widely in SE Asia and adjacent oceans. The Semilir eruption could have triggered a climate response, but cannot yet be linked with certainty to Early Miocene climatic events such as glaciations.

Keywords: East Java, Miocene Eruption, U-Pb

1 Introduction

Indonesia is well known for spectacular volcanic activity, including the 1883 eruption of Krakatau, Java, the 1815 eruption of Tambora, Flores, and the 74 ka eruption of Toba, Sumatra (Fig. 1). Intriguingly, there are no records of earlier, pre-Pleistocene, large eruptions from SE Asia despite the long history of subduction along the Indonesian archipelago (Hall, 2002). Mason et al. (2004) reported large eruptions from New Zealand, Australia, Africa, and North and South America but none from SE Asia and proposed that there were two major Cenozoic global eruptive pulses from 36 to 25 Ma and 13.5 to 0 Ma. However, it is notable that 33 of the largest 47 eruptions listed by Mason et al. (2004) are from North America and it is not clear if the lack of a record from SE Asia reflects an absence of large eruptions, or a comparative lack of work in a relatively understudied tropical region. On the basis of the study reported in this paper we suggest the latter is the case. We present evidence for a very large Early Miocene eruption in Java, the Semilir event, which occurred between the pulses identified by Mason et al. (2004) and appears comparable in size to the 74 ka eruption of Toba in Sumatra.

Volcanic eruptions, especially large events, are an important natural cause of climate change (Robock, 2000) as they inject huge volumes of ash and gases into the atmosphere. The Quaternary eruptive history of some of SE Asia's numerous volcanoes is well-known. The 1815 eruption of Tambora resulted in the "year without a summer" in 1816 (Harington, 1992; Oppenheimer, 2003; Stommel and Stommel, 1983; Zeilinga de Boer and Sanders, 2002). Furthermore, the Late Pleistocene Toba eruption, the largest magnitude explosive eruption in the last million years, has been suggested by some

workers to have accelerated Pleistocene global cooling as it occurred during the interval of most rapid ice accumulation in the last glacial cycle (Rampino and Self, 1992). The 74 ka eruption of Toba is thought to have expelled 2800 km^3 of material, 800 km^3 of which was deposited as ash fall (Oppenheimer, 2002; Rose and Chesner, 1987; Song et al., 2000). It has been suggested that the event led to a human population bottleneck due to a climate deterioration (Lee et al., 2004; Rampino and Self, 1993a), but other workers have argued that the eruption had little effect on mammal populations (Ambrose, 2003b; Gathorne-Hardy and Harcourt-Smith, 2003; Louys, 2007; Oppenheimer, 2002), including humans (Petraglia et al., 2007). The Greenland ice core records include a major sulphur anomaly associated with the 74 ka Toba eruption, but recent models suggest the eruption had no long term effect on climate (e.g., Oppenheimer, 2002). We discuss the possibility that the Semilir eruption influenced climate in the Early Miocene.

2 Geological background

Java is between Asia and Australia at the centre of the Indonesian archipelago (Fig.1) where the Indo-Australian Plate subducts beneath the Eurasian Plate. There has been subduction at the Java Trench since the Early Cenozoic (Hall, 2002; Smyth et al., 2008b). The almost east-west elongation of the island follows the Benioff zone contours and most of the active volcanoes on Java are situated about 100 km above the subducting slab (England et al., 2004). The present-day volcanic chain, which forms the elevated axis of the island (Fig. 2a), has been active since the Late Miocene (Soeria-Atmadja et al., 1994) and is part of the Sunda Arc. An Eocene to Early Miocene volcanic arc in East Java, the

Southern Mountains Arc (Smyth, 2005), is parallel to and south of the modern arc (Figs. 1 & 2). Thick volcanic and volcaniclastic deposits related to this arc are well preserved in East Java and identified volcanic centres are separated by similar distances to volcanoes of the modern arc (Smyth et al., 2008a). However, unlike the modern Sunda Arc, the Southern Mountains Arc was a chain of small volcanic islands separated by intra-arc basins (Fig. 2c).

2.1 Geology of the Southern Mountains of East Java

New field investigations and stratigraphic studies (Smyth, 2005; Smyth et al., 2008b) in East Java have identified the most important features of arc activity in the Southern Mountains. The oldest sedimentary rocks are conglomerates and sandstones that lack volcanic material and were deposited unconformably on a basement that included ophiolitic and continental rocks (Smyth et al., 2008b; Smyth et al., 2007). In the overlying sedimentary rocks volcanic debris and detrital zircons indicate initiation of the arc, and subduction beneath Java, by the Middle Eocene (42 Ma) (Hall and Smyth, 2008; Smyth et al., 2008a). The arc was active until the Early Miocene (18 Ma) and volcanic activity was most abundant during the Oligocene to Early Miocene. In contrast to present-day Java, the Southern Mountains Arc was a chain of small volcanic islands (Fig. 2c) surrounded by carbonate and volcaniclastic shelves, separated by intra-arc basins, resembling the present day Izu-Bonin-Mariana arc and the Aleutian Islands (Smyth, 2005; Smyth et al., 2005; Smyth et al., 2008b). Volcanic activity was commonly explosive and of Plinian-type (Smyth et al., 2008b; Soeria-Atmadja et al., 1994). The

erupted products range from andesite to rhyolite (Fig. 2d) and formed lava flows, lava domes, volcanic breccias and extensive pyroclastic deposits including flow, air-fall and surge deposits (Smyth et al., 2008b; Soeria-Atmadja et al., 1994). Volcanic activity along the Southern Mountains Arc culminated in the Early Miocene in a climactic phase of eruptions preserved in the Batu Agung Escarpment, near Yogyakarta (Smyth et al., 2008b). It was during this climactic phase that the Semilir Eruption occurred.

2.1.1 Stratigraphy of the Batu Agung Escarpment

In the area around Yogyakarta, southern East Java (Figs. 2 & 3), there are thick sections of volcanic and sedimentary rocks recording the final stages of volcanic activity in the Southern Mountains Arc. In this region, north-flowing rivers dissect the steep northern flank and the gently dipping southern slope of the Batu Agung Escarpment (Fig. 2a) to expose over 2000 m of almost continuous section. The volcanic deposits are fresh and dip uniformly towards the south at approximately 30º. The sequence is divided into three formations (Rahardjo et al., 1995; Surono and Sudarno, 1992) which are, from base to top, the Kebobutak, Semilir and Nglanggran Formations (Fig.3). They are overlain by a sequence of reworked volcanogenic and carbonate rocks assigned to the Sambipitu, Kepek and Wonosari Formations (Fig.3) (Harahap et al., 2003; Rahardjo et al., 1995; Surono and Sudarno, 1992).

The Kebobutak Formation is exposed at the base of the northern flank of the escarpment and consists of at least 400 m of interbedded rocks that were deposited as crystal-rich volcaniclastic sands, tuffaceous muds and mantling ashes. Upper bedding surfaces are intensely bioturbated by a *Cruziana*-type assemblage. The formation is interpreted to be

air-fall deposits reworked in a shallow marine sub-littoral setting (Smyth et al., 2008a). Conformably above the Kebobutak Formation lies at least 600 m of dacitic pumice, volcanic lithic and crystal-rich tuffs and breccias assigned to the Semilir Formation (Fig. 3). Unlike the underlying Kebobutak Formation there is very little bioturbation and little evidence of reworking in the Semilir Formation. In tropical settings such as those of Java it is often difficult to trace formation boundaries due to the lack of continuous, unweathered exposure. However, in East Java the base of the Semilir Formation can be identified by the abrupt termination of bioturbated reworked deposits characteristic of the Kebobutak Formation. The volcanic rocks of the Semilir Formation are characterized by features typical of terrestrial air-fall, pyroclastic surge and flow deposits including dune and antidune structures, crystal layering, well-sorted granular laminations, diffuse bedding, breccias (with metre-scale pumice blocks), thick mantling ashes, and abundant fragments of charcoal. Locally there are water-laid deposits, with scoured irregular bases, flame, traction and suspension structures, and large slump folds indicating an unstable marine slope. We interpret these observations to indicate the Semilir Formation was erupted in a subaerial setting in which pyroclastic flows travelled across vegetated slopes picking up and baking plant fragments, with some of these flows entering the sea. Some of the primary material would have been redeposited as lahars in distal settings.

Overlying the Semilir Formation is a 200 to 500 m thick sequence of massive, resistant, monomict andesitic volcanic breccias (Fig. 3f & g), crystal-rich sandstones and minor lava flows of the Nglanggran Formation. The breccia beds are 1 to 10m thick and can be mapped for several kilometres. Interbedded crystal-rich sandstones are much thinner. The

breccias are both clast- and matrix-supported with angular fragments commonly 2 to 75 cm across with some blocks up to 3 m. Fragment imbrication within the breccias records diverging west and southwest flow from a source in the northeast part of the Batu Agung Escarpment. There is no evidence of any marine influence, and we interpret the Nglanggran Formation as terrestrial deposits formed by sector or repeated dome collapse, marking the end of arc activity in the Southern Mountains. The top and base of the Nglanggran Formation forms topographic breaks in slope, because the andesitic breccias are much more resistant than the underlying and overlying units, and the feature and the formation can be easily mapped across the area over a distance of 46 km.

Based on examined exposures, measured sections and published geological maps, the combined thickness of the Semilir and Nglanggran Formations is between 250 and 1200 m, exposed over 800 km^2, and the total volume of volcanic material at least 480 km^3.

Conformably overlying these primary volcanic deposits are calcareous volcanogenic turbidites of the Sambipitu Formation (Fig. 3c). This formation records the erosion, submergence, subsidence and reworking of the volcanic deposits of the extinct Southern Mountains Arc in a deep marine setting. The formation represents a time interval of approximately 10 million years (based on identifications made by Kadar, 1986). At the top of the Sambipitu Formation there are several unreworked ash beds which mark the resurgence of volcanic activity in the Late Miocene. The formation is laterally equivalent to the Wonosari Formation, a carbonate platform which formed a fault-bounded high in nearby south Java. In places the Wonosari Formation onlaps the Semilir and Nglanggran Formations (Fig.3b).

The entire sequence (Kebobutak, Semilir, Nglanggran and Sambipitu Formations) has previously been suggested to range in age from Late Oligocene to Middle Miocene, and the Semilir and Nglanggran Formations to be of Early to Middle Miocene age (N5-N9: 21.2–14.2 Ma) based on microfossils from unidentified localities (Harahap et al., 2003; Kadar, 1986; Rahardjo et al., 1995; Surono and Sudarno, 1992). However, in the many sections of the Batu Agung Escarpment examined in this study, the Semilir and Nglanggran Formations consist entirely of non-fossiliferous volcanic rocks with no significant break within or between the formations. Zircons from the succession were dated using SIMS (Secondary Ion Mass Spectrometry). This was part of a larger programme of reconnaissance dating across Eastern Java (Smyth et al., 2007). This initial analysis (e.g., sample Jhs3PRAMB Smyth et al., 2007) indicated that the entire Semilir Formation could have been deposited in a very short period in the Early Miocene. Additional samples were collected through the formation in order to date the sequence. Zircons separated from these samples were first analysed using SIMS and then by ID-TIMS (Isotope Dilution-Thermal Ionization Mass Spectrometry) in order to achieve a higher level of precision.

2.2 Age of the Semilir and Nglanggran Formations

2.2.1 Methods

2.2.1.1 SIMS

Zircon grains separated from rock samples were mounted in resin blocks together with pieces of zircon standard CZ3, and imaged using cathodoluminescence (CL) on a Philips XL30 SEM prior to isotopic analysis by SHRIMP-II at the John de Laeter Centre, for Mass Spectrometry, Western Australia. SIMS was the dating method used in our first detailed study of the Semilir Formation (Smyth et al., 2007). Our previous work in Java had highlighted the presence of ancient inherited cores in many zircons from volcanic rocks (Smyth, 2005; Smyth et al., 2007).

A selection of the CL images, used to guide analytical spot selection, is provided in Figure 4. Generally, domains characterised by simple oscillatory zoning were selected for analysis, avoiding structural cores and other areas of complexity, inclusions, resorption and/or recrystallization. Operating conditions for SHRIMP analyses were routine, namely 25 μm analytical spot size, primary beam current 2-3 nA, mass resolution 5000 (1% valley) and sensitivity for Pb isotopes ≥ 12 cps/ppm/nA. Pb/Pb and Pb/U isotopic ratios and U, Th and Pb concentrations were measured in 20 minute, 7-scan duty cycles. Data for Semilir samples Jhs4SEM 1-7 were acquired in a continuous 36 hr analytical session, interspersed with sixteen analyses of zircon standard CZ3. The remaining samples were run separately but under similar conditions. Because of the young age of the rocks, correction of isotope ratios for common Pb was based on the measured ^{208}Pb, with the common Pb composition modelled upon that of Broken Hill ore Pb. Pb/U isotopic ratios were also corrected for instrumental inter-element discrimination using the method of Compston *et al.* (1992) in which the measured ratios are normalized via a calibration curve to analyses of the zircon standard. Data were processed using PDK's

KRILL software and ISOPLOT 3 (Ludwig, 2003). The normalizing $^{206}Pb/^{238}U$ ratio used for CZ3 was 0.0910 (561.5 Ma), which is a recently revised value (previously 0.0914, 564 Ma). Ages were calculated using standard U-Pb decay constants (Jaffey et al., 1971). Uncertainties in ages of individual spot analyses are quoted as 2σ values (Supplementary data table).

2.2.1.2 TIMS

In addition to the SIMS dating, two samples (Jhs4SEM4 and Jhs4SEM7) were selected for dating by isotope dilution thermal ionization mass spectrometry (ID-TIMS). ID-TIMS yields the highest analytical precision of any U-Pb dating technique; it was utilised here to assess the preliminary results from SIMS dating in order to determine if different levels of the volcanic Semilir Formation were produced by several separate eruptive events, or whether the formation as a whole formed within a time-frame less than that which can be resolved by the technique. Zircons were thermally annealed and leached by a process modified from that of Mattinson (2005). Zircons were annealed as bulk fractions at 850°C in quartz glass beakers for 60 hours. Once cooled, the zircon crystals were ultrasonically washed in 4N HNO_3, rinsed in ultra-pure Milli-Q water, then further washed in warm 4N HNO_3 prior to rinsing with water to remove surface contamination. The annealed and cleaned zircon fractions were then chemically leached in Teflon microcapsules enclosed in a Parr bomb using 200µl 29N HF and 20µl 8N HNO_3 at 180°C for 12 hours. This procedure was carried out in order to minimise or eliminate damaged zones in which Pb loss may have occurred. Zircons were then hand picked avoiding any grains with obvious inherited cores or inclusions.

A mixed ^{205}Pb – ^{233}U – ^{235}U EARTHTIME tracer was used to spike all fractions, which once fully dissolved, were converted to chloride and loaded onto degassed rhenium filaments in silica gel, following a procedure modified after Mundil *et al.* (2004). A Thermo Electron Triton at the Natural Environment Research Council (NERC) Isotope Geosciences Laboratory (NIGL) was used to collect all U-Pb TIMS data. Approximately 100 to 150 ratios of Pb isotopic data were dynamically collected using a new generation of MassCom Secondary Electron Multiplier (Noble et al., 2006). Between 60 to 80 ratios were statically collected using Faraday cups for U. Pb ratios were scrutinised for any evidence of organic interferences using an in-house raw ratio statistical and plotting software, but these were found to be negligible or non-existent. Errors were calculated using numerical error propagation (Ludwig, 1980). Isotope ratios were plotted using Isoplot version 3.63 (Ludwig, 1993; Ludwig, 2003); error ellipses on concordia diagrams (Fig.5) reflect 2σ uncertainty. Total procedural blanks were 1.0 pg for Pb and ca. 0.1 for U. Samples were blank corrected using the measured blank composition. Correction for residual common lead above analytical blank was carried out using the Stacey-Kramers common lead evolutionary model (Stacey and Kramer, 1975).

2.2.2 Results

The sample location data are summarised in Table 1 and results obtained from the SIMS method are provided in the supplementary data table and plotted on Figure 5. ID-TIMS data are presented in Table 2 and Figure 6.

The Kebobutak Formation underlies the Semilir Formation. This formation is not a primary volcanic deposit but rather an epiclastic succession. Reworking, clearly seen in

outcrop, petrographic examination, and in the biostratigaphy, it is also observed in the age range of the zircons from two samples (Smyth, 2005). Zircons were analysed from two volcaniclastic sandstones, close to the base of the Kebobutak Formation, underlying the Semilir Formation. The ranges in zircon SIMS spot ages for the two samples were 30.2 ± 2.5 to 21.1 ± 3.6 Ma (Jhs2JKB21), and 32.2 ±2.2 to 24.7 ± 1 Ma (Jhs2Sat1) (Smyth, 2005). Other samples from the upper parts of the Kebobutak Formation were either too fine grained or yielded too few zircons for dating. The range of zircon ages (SIMS data) suggests mixing of material from a number of eruptions. Reassessment of the data presented by Harahap et al. (2003) show the presence of planktonic foraminifera age markers *Paragloborotalia kugleri*, *Globigerinoides primordius*, *Globigerinoides trilobus* and *Globoquadrina binaiensis,* indicating an Early Aquitanian age and planktonic foraminiferal zone N4, between 23-20.5 Ma (Marcelle BouDagher-Fadel pers. comm.). Unfortunately, Harahap et al. (2003) do not provide information on numbers of samples examined, sample locations or lithological descriptions. The majority of Kebobutak Formation samples examined in this study did not yield any bioclasts.

Five tuffs from the base (Jhs4SEM2), middle (Jhs4SEM5, 4 and 7) and top (Jhs4SEM1) of the Semilir Formation (Fig. 3c), yielded euhedral and elongate prismatic zircons (Fig. 4). As the grains analyzed are geologically young, and therefore do not contain abundant radiogenic Pb, and several grains have experienced Pb loss, a ^{208}Pb correction could potentially add uncertainties to the calculated age. The uncorrected lower intercept was therefore chosen as the most suitable method of sample age calculation. Regardless of stratigraphic position, SHRIMP ages for samples of the Semilir Formation are within

error of each other. In stratigraphic order from base to top these are 20.6 ± 0.5, 20.8 ± 0.5, 20.7 ± 0.6, 20.9 ± 0.5 and 20.0 ± 0.6 Ma (uncorrected $^{206}Pb/^{238}U$ weighted mean ages with 2σ error are shown in Supplementary data table and Fig. 5). The stratigraphically lowest sample (Jhs4SEM2) contains a number of older grains that may be xenocrysts (Fig.5), and which may reflect protracted growth in the magma chamber preceding eruption (as discussed in Reid, 2008).

Samples Jhs4SEM4 and Jhs4SEM7 were selected for ID-TIMS analysis (Fig. 6, Table 2) in order to achieve a higher precision age and test the hypothesis that the Semilir Formation was erupted in a single recognisable event. The small size of the zircons and their low radiogenic Pb concentrations favoured analyses of multi-grain fractions. Analyses display radiogenic to common Pb ratios (Pb*/Pb) of 4 to 14 with between 11 and 30pg of radiogenic Pb (Pb*). Intermediate decay products in the U-Pb decay chains have been taken into consideration. Magmatic processes are not known to result in fractionation of ^{234}U from ^{238}U and the effect of ^{231}Pa on U-Pb systematics in zircon appears to be an extremely rare phenomenon only reported from pegmatites (e.g., Anczkiewicz et al., 2001). The presence of ^{232}Th, however may significantly affect measured U/Pb ratios. Disequilibrium between minerals and magma was quantified using concentration ratios and the formula: $f = [Th/U]_{mineral} / [Th/U]_{magma}$. The $[Th/U]_{mineral}$ was obtained from measured radiogenic ^{208}Pb and the uranium isotope dilution measurements for each zircon fraction. $[Th/U]_{zircon}$ ranges from 0.75 to 0.85 and for samples Jhs4SEM4 and Jhs4SEM7. Th/U will decrease with increasing magmatic differentiation, so finding an appropriate $[Th/U]_{magma}$ can be problematic in that any measured Th/U from the final products of crystallisation or from volcanic glass may differ from the $[Th/U]_{magma}$ at the

time when zircon was crystallising in the paragenetic sequence. Dacites typically have a Th/U 2.8 to 3.3, but variations outside this range are known (e.g., Zartman and Cunningham, 1995). For example, Alves et al. (1999) state that Miocene volcanic rocks from Java have an anomalously high Th/U ratio of ca 4.2 which may be due to the pre-diagenetic preferential leaching of U relative to Th in sedimentary material entering the subduction zone and influencing the resultant composition of subduction-related lavas. The ages reported below use a $[Th/U]_{magma} = 4.0$, which is considered the best estimate of magma composition at the time of zircon crystallisation because it is a value slightly below that of the fully crystallised Miocene andesites and dacites from Java (Alves et al., 1999). Taking an extreme range of $[Th/U]_{magma}$ from 2.8 to 4.5 results in only a ca 11 k.y. (0.05%) difference in the ^{230}Th-corrected $^{206}Pb/^{238}U$ mean ages for samples JhsSEM4 and JhsSEM7. For sample JhsSEM4, five zircon fractions give a mean $^{206}Pb/^{238}U$ age of 20.69±0.05, but with a high degree of scatter probably due to some residual Pb-loss. Three fractions (Z1, Z2 and Z5) give a more robust mean $^{206}Pb/^{238}U$ age of 20.72±0.02 (MSWD = 0.71, probability = 0.49). The remaining three zircon fractions for JhsSEM4 yield analyses indicative of older components with $^{206}Pb/^{238}U$ ages between 21.23±0.03 and 21.72±0.02 Ma. Two out of five fractions from sample JhsSEM7 (Z1 and Z5) give $^{206}Pb/^{238}U$ ages which overlap within error of the ca. 20.7 cluster from sample JhsSEM4. When combined, the seven fractions give a mean $^{206}Pb/^{238}U$ age of 20.73±0.02 Ma (MSWD = 0.48, probability = 0.75). Zircon fraction Z1 from sample JhsSEM7 is the only single grain fraction analysed from either sample and gives a $^{206}Pb/^{238}U$ age of 20.74±0.05 Ma. The remaining fractions from sample JhsSEM7 give older $^{206}Pb/^{238}U$ ages ca. 21-22 and ca. 25 Ma.

In the case of both samples dated by ID-TIMS, older zircon fractions may be evidence either for zircon growth in a pre-eruptive magma-chamber, or alternatively may represent partially assimilated products of older magmatism (i.e., xenocrysts / antecrysts) at the site of the Semilir eruption. CL images of representative grains from each of the dated samples (Fig. 3) demonstrate complex zones of resorption and or overgrowth. Some of these textures are likely to have resulted from magmatic overgrowths on xenocrystic cores (e.g., Fig. 3), but some of the CL images display subtle disequilibrium textures (partial resorption and truncated magmatic zoning) which may have a different origin. Nevertheless, although disequilibrium textures are common in the imaged zircons, a cluster of four multi-grain fractions and one single grain fraction give a weighted mean $^{206}Pb/^{238}U$ age of 20.72±0.02 Ma. This suggests that if these textures reflect protracted magma chamber residence and associated chemical disequilibrium of separate magma pulses, the duration of this process is less than 20 ka (i.e., the 2σ error calculated from ID-TIMS ^{230}Th-corrected $^{206}Pb/^{238}U$ ages). With the exception of Mount St. Helens, where zircons record protracted magma storage durations in the order of hundreds of thousands of years (Claiborne et al., 2010), most known examples of magma chamber residence, as deduced from variations in U-Pb zircon ages, are generally less than 800 ka (e.g., ca 500 ka for the youngest Toba tuff (Reid, 2008)) and generally much less than 20 ka e.g., Bishop Tuff, Crowley et al. (2007). It is therefore likely that the apparent U-Pb ages older than 20.7 Ma represent inherited xenocrystic zircon components. Given the low MSWD of five zircon fractions from two separate samples, we interpret 20.72±0.02 Ma as being the best estimate for a final eruptive event which generated the Semilir Formation.

The Nglanggran Formation samples contained no zircons but its age is constrained by biostratigraphic dating of turbidites from the overlying Sambipitu Formation (Kadar, 1986) which span the nannofossil zones NN2-NN8 corresponding to 22.8–10.5 Ma (Lourens et al., 2004). Re-examination of the data of Kadar (1986) shows that a sample 100 m above the base of the formation can be precisely dated by the first occurrence of the short-lived species *Globigerina binaensis* as 20-19.1 Ma. The Nglanggran Formation must therefore be older than 19 Ma.

3 Distribution of the ash deposits

The Semilir and Nglanggran Formations were deposited very close to an active volcanic centre that must have been near the Batu Agung Escarpment (Fig. 3) based on the character of the erupted material. The U-Pb zircon ages and fossil evidence indicate that the entire 1200 m succession was deposited in an interval of less than one million years. The U-Pb ID-TIMS zircon data for the Semilir Formation indicates that two samples record events with a duration of less than 50 ka which were likely to have been a single eruptive event. We suggest that the eruption was Toba-scale but not Toba-type as discussed below.

3.1 Influence of tropical weathering

The study area is today located just to the south of the equator (~8°S), as it was

throughout much of the Cenozoic (Hall, 2002). Therefore the influence of tropical weathering must be taken into consideration when assessing the preservation and distribution of the products of the Semilir Event. Tropical weathering would have altered the strata during the eruption, immediately after deposition, and today, at intervals when they were exposed at the surface. Tropical environments with high temperatures and precipitation rates are sites of rapid weathering and erosion (Dosseto et al., 2006; White and Blum, 1995). Unconsolidated volcanic deposits and sediments which are subject to tropical weathering would be expected to break down much more rapidly than lithified sediments or resistant igneous rocks such as granite. It is generally accepted that tropical climatic settings will have higher rates of chemical disaggregation of source rocks and resultant daughter products than in high latitude settings.

The 1883 eruption of Krakatau is an excellent case study which shows how rapidly products of an eruption, exposed to tropical conditions, can be removed by tropical weathering. The cataclysmic eruption of 27th August destroyed much of Krakatau Island, but thick ash and pumice deposits created new land area. However, by October 1883, some three months after the eruption, much of the new land area that was created by the thick volcanic deposits had been lost, and the new islands of Steers and Calmeyer and the islet off eastern Sertung had disappeared (Thornton, 1996). In subsequent decades the slopes of the remnant volcanic edifice were stabilised by vegetation, soil profiles developed and altered by renewed volcanism from Anak Krakatau, but the sedimentation rates in the area were still high with rates of between 1 – 3.5 m/year reported (Thornton, 1996 and references therein). This modern, well-studied, example serves to show how

quickly the volcanic products can be reworked and the record of major events could potentially be lost.

The absence of significant weathering or gully formation, lack of soil profiles or bioturbation within the thick ash pile that comprises the Semilir Formation suggests that they are the products of a single event. These labile ashes must have been covered immediately, or soon after their deposition, by the coarse resistant andesitic breccias of the Nglanggran Formation, which protected the ashes from further alteration.

3.2 Comparison with the scale of the 74 ka of Toba

To assess the importance of this eruption, we compared the products with the most proximal deposits of Toba in Sumatra (Figs. 1 & 7). It should be noted that we are comparing the scale of the eruption rather than the type of the eruption. The Semilir volcanic centre is interpreted to have been an isolated volcanic island, and part of an island arc chain (Fig. 2), whereas Toba was located within an extensive emergent land area within a chain of volcanoes on Sumatra (Gasparon, 2005). Many of the volcanic products would therefore be different. Toba erupted over an interval of about 1.2 million years with 4 events known at 1.2 Ma, 840, 501 and 74 ka (Chesner et al., 1991).

The time span of eruptive activity, thicknesses, area and estimated volumes of volcanic deposits in the vicinity of the Toba volcanic centre are similar to those at Semilir (Fig. 7). Considering the much greater age of the Semilir and Nglanggran Formations, the effects of compaction and erosion, duration and intensity of tropical weathering, and the likely

extent of unobserved parts of the formations now covered unconformably by younger rocks, these observations suggest an eruptive event comparable in magnitude to the Pleistocene eruptions of Toba. Most of the volcanic rocks preserved near Toba are the product of the 74 ka event, and it is likely that the Batu Agung succession is also mainly the product of a climactic eruption because of its proximity to the volcanic centre.

Material from the 74 ka eruption of Toba is distributed over a very large area west of Sumatra, including eastern India and the Indian Ocean seafloor, and was dispersed by prevailing winds at the time of eruption (Chesner et al., 1991; Song et al., 2000). Such a large scale eruption would have transported vast amounts of the finer particles straight into the stratosphere and, due to its near equator position, the material would have been transported across both hemispheres (Bains and Sparks, 2005). The larger particles would have been predominantly transported by the local winds. Unfortunately, the pattern of atmosphere circulation during the Early Miocene cannot be determined. In addition, finding a record offshore is likely to be difficult because about 1300 km of ocean crust (Fig. 8) has been subducted at the Java Trench since 20 Ma (Hall, 2002). Using the distributions of Neogene tephra from Toba as a guide suggests that if ash had been carried west or south all but the most distal material would have been subducted or would be difficult to identify in deformed accretionary complexes (Fig.8). However, if material had been carried east or north it could be preserved on land, offshore on the Australian NW Shelf, or in basins of SE Asia.

There are many unusual, compositionally mature but texturally immature, widely distributed volcanic quartz-rich sandstones of Early Miocene age exposed in East Java

that may be Semilir products but have not been precisely dated. One such sandstone is the Jaten Formation, exposed near Pacitan, 80 km east of the Batu Agung Escarpment (Fig. 2.). The location and character of this formation are described in detail in Smyth et al. (2008a, b). Zircons from the Jaten Formation have a weighted mean SIMS age of 19.6 ± 0.5 (MSWD 0.22, Smyth et al., 2005) and this is consistent with them being reworked products of the Semilir eruption. Other quartz-rich sandstones from Java have not yet been dated using U-Pb methods.

Published records of sedimentary basins drilled for hydrocarbons provided insufficient detail to identify volcanic ash. However, in the deeper marine areas there is volcanic material which is the correct age and composition at DSDP and ODP sites near the NW Shelf (Sites 260, 760, 762, 765, 766), Celebes Sea (Site 767) and South China Sea (Site 1148) (Figure 1). Unfortunately the stratigraphic resolution of the critical time interval at these sites is insufficient to identify Semilir eruptive products with certainty.

3.3 Impact of the eruption

The impacts of major eruptions, such the 74 ka eruption of Toba, are the subject of some debate. Smaller modern analogues have been used to suggest that all life in the immediate vicinity of the crater would have been destroyed (Gathorne-Hardy and Harcourt-Smith, 2003) but would recover very quickly (e.g., Thornton, 1996).

The climatic consequences are even more uncertain. While it has been speculated that eruption of Toba led to a “volcanic winter”, accelerated glaciation and a bottleneck in

human evolution (Ambrose, 2003a; Rampino and Self, 1992; Rampino and Self, 1993a; Rampino and Self, 1993b), others suggest that the impact on mammalian populations, including humans, was much less severe (Gathorne-Hardy and Harcourt-Smith, 2003; Louys, 2007; Oppenheimer, 2002; Petraglia et al., 2007). Recent archaeological studies, based on archaeological finds and tephra chronology, suggests that hominids persisted, rather than perished (Petraglia et al., 2007). Ash and gases would have been transported into the stratosphere and subsequently dispersed from their equatorial origin via Walker Circulation (Rietmeijer, 1993; Trepte and Hitchman, 1992) to higher latitudes but the distribution of coarse particulates are strongly influenced by the prevailing wind direction (Bühring et al., 2000; Chen et al., 2000). Eruption foot-print maps of Toba (e.g., Chen et al., 2000; Miller and Wark, 2008; Song et al., 2000) show that most of the material was transported towards the west into the Indian Ocean and to the Asian sub-continent. The distribution of material erupted by the Semilir event is not known but the broad similarities of palaeogeography (Hall, 2002) suggest a pattern similar to that of Toba's products is plausible (Fig. 8).

Semilir's products, notably the sulphur aerosols, would have reflected sunlight and cooled the Earth like those the Mount Pinatubo eruption (e.g., Robock, 2000). The Early Miocene was an interval of general global warmth, interrupted by several large-scale Antarctic glaciations (Wright et al., 1992). The major glaciation, Mi1, at 23 Ma predates the Semilir eruption. The time of the Semilir eruption is an interval associated with an increase in $\delta^{18}O$ values of benthic foraminifers, indicating cold climates and/or an increase of ice build up, of a similar magnitude to that recorded during Mi1 (Pälike et al.,

2006). The shift in $\delta^{18}O$ at the time of eruption of Semilir coincides with a low eccentricity associated with the 400-ky astronomical cycle and additionally the 40-ky obliquity cycle. It is possible that a very high resolution analysis of the amplitude and duration of this cycle, indicating abnormalities compared to previous events, could identify influences of the Semilir eruption on Early Miocene climate. However, the Early Miocene was also a time of other important changes, such as tectonic restriction of the oceanic gateway between the Pacific and Indian Oceans (Kuhnt et al., 2004) and the rise of mountains due to Australia-SE Asia collision (Hall, 2002), which are also likely to have had a climatic impact. Any potential relationship between the length and amplitude of glaciations and the Semilir eruption should be tackled in the future by combining regional and temporal climate patterns with additional radiometric dating.

4 Conclusions

The deposits of the Semilir Formation were erupted at 20.72 ± 0.02 Ma and the Nglanggran Formation was deposited soon afterwards, before 20 Ma. The Semilir eruption is the first pre-Pleistocene record of a Toba-scale event in SE Asia despite the long history of volcanism in this region. This suggests that the absence of a record of large eruptions in Indonesia (and possibly more widely in the west Pacific) is a reflection of preservation, rapid tropical weathering and sampling rather than diminished volcanic activity. Indonesia, SE Asia and the West Pacific remain understudied compared to other regions, notably North America, from which most of the very large eruptions have been recorded. The products of the Semilir eruption may have covered large parts of SE

Asia and adjacent oceans. Large eruptions are known to influence global climate and an event such as Semilir could certainly have triggered a climate response, but the eruption and climatic consequences such as Early Miocene glaciations cannot yet be linked with certainty.

5 Acknowledgements

This project was funded by the SE Asia Research Group at Royal Holloway, supported by an oil company consortium. Reconnaissance SIMS dating was supported by CSIRO, Australia, and the SHRIMP dating of the six Semilir samples was funded by a grant from the University of London Central Research Fund. Technical support at NIGL was provided by Aaran Sumner and Neil Boulton. We thank LIPI Indonesia, Eko Budi Lelono, Peter Lunt, Wolfgang Müller, Colin Macpherson and Heather Handley. DNS acknowledges funding from the Royal Society via a University Research Fellowship. The authors which to thank the anonymous reviewers for their helpful comments which improved the manuscript.

6 References

Alves, S., Schiano, P. and Allégre, C.J., 2004. Rhenium-osmium isotopic investigation of Java subduction zone lavas. Earth and Planetary Science Letters 168, 65-77.

Ambrose, S.H., 2003a. Did the super-eruption of Toba cause a human population bottleneck? Reply to Gathorne-Hardy and Harcourt-Smith. Journal of Human Evolution

45, 231-237.

Ambrose, S.H., 2003b. Did the super-eruption of Toba cause a human population bottleneck? Reply to Gathorne-Hardy and Harcourt-Smith. Journal of Human Evolution 45, 231-237.

Anczkiewicz, R., Oberli, F., Burg, J.P., Villa, I.M., Günther, D. and Meier, M. 2001. Timing of normal faulting along the Indus Suture in Pakistan Himalaya and a case of major $^{231}Pa/^{235}U$ initial disequilibrium in zircon. Earth and Planetary Science Letters 191, 101-114.

Bains, P.G. and Sparks, R.S.J., 2005. Dynamics of giant volcanic ash clouds from supervolcanic eruptions. Geophysical Research Letters 32 (L24808).

Bühring, C., Sarnthein, M. and Party, L.S.S., 2000. Toba ash layers in the South China Sea: Evidence of contrasting wind directions during eruption ca. 74 ka. Geology 28, 275-578.

Chen, C.H., Yang, T.F., Song, S.R., Iizuka, Y. and Wei, K.-Y., 2000. Toba ash layers in the South China Sea: Evidence of contrasting wind directions during eruption ca. 74ka: Comment and Reply. Geology 28, 1055-1056.

Chesner, C.A., Rose, W.I.., Deino, A., Drake, R. and Westgate, J.A., 1991. Eruptive history of Earth's largest Quaternary caldera (Toba, Indonesia) clarified. Geology 19, 200-203.

Claiborne, L.L., Miller, C.F., Flanagan, D.M., Clynne, M.A. and Wooden, J.L., 2010.

Zircon reveal protracted magma storage and recycling beneath Mount St. Helens. Geology 37, 1011-1014.

Compston, W., Williams, I.S., Kirschvink, J.L., Zichao, Z. and Guogan, M.A., 1992. Zircon U-Pb ages for the Early Cambrian time-scale. Journal of the Geological Society of London 149, 171-184.

Dosseto, A., Bourdon, B., Gaillardet, J., Allegre, C.J. and Filizonla, N., 2006. Time scale and conditions of weathering under tropical climate: Study of the Amazon basin with U-series. Geochimica et Cosmochimica Acta. 70, 71-89.

England, P., Engdahl, R. and Thatcher, W., 2004. Systematic variation in the depths of slabs beneath arc volcanoes. Geophysical Journal International 156, 377-408.

Gasparon, M., 2005. Quaternary volcanicity in Barber, A.J., Crow, M.J. and Milson, J. (Eds.), Sumatra: geology, resources and tectonic evolution. Geological Society of London Memoirs. Geological Society of London, Bath, pp. 120-130.

Gathorne-Hardy, F.J. and Harcourt-Smith, W.E.H., 2003. The super-eruption of Toba, did it cause a human bottleneck? Journal of Human Evolution 45, 227-230.

Hall, R., 2002. Cenozoic geological and plate tectonic evolution of SE Asia and the SW Pacific: computer-based reconstructions, model and animations. Journal of Asian Earth Sciences 20, 353-434.

Hall, R. and Smyth, H.R., 2008. Cenozoic arc processes in Indonesia: Identification of the key influences on the stratigraphic record in active volcanic arcs in Draut, A., Clift,

P.D. and Scholl, D.W (Eds.), Formation and Applications of the Sedimentary Record in Arc Collision Zones. Special Paper. Geological Society of America, Boulder, pp. 27-54.

Harahap, B.H., Bachri, S., Baharuddin, S.N., Panggabean, H. and Simanjuntak, T.O., 2003. Stratigraphic lexicon of Indonesia. Geological Research and Development Centre, Indonesia, Bandung.

Harington, C.R. (Ed), 1992. The year without a Summer: World Climate in 1816. Canadian Museum of Nature, Ottawa.

Jaffey, A.H., Flynn, K.F., Glendenin, L.E., Bentley, W.C. and Essling, A.M., 1971. Precision measurement of half-lives and specific activities of 235U and 238U. Physics Reviews 4, 1889-1906.

Kadar, D., 1986. Neogene planktonic foraminiferal biostratigraphy of the south central Java area, Indonesia, Special Publication 5, Geological Research and Development Centre, Bandung. .

Knight, M.D., Walker, G.P.L., Ellwood, B.B. and Diehl, J.F., 1986. Stratigraphy, paleomagnetism, and magnetic fabric of the Toba Tuffs: constraints on the sources and eruptive styles. Journal of Geophysical Research 91, 10355-10382.

Kuhnt, W., Holbourn, A., Hall, R., Zuvela, M. and Käse, R., 2004. Neogene history of Indonesian Throughflow, in: Clift, P., Hayes, D., Kuhnt, W. and Wang, P. (Eds), Continent-Ocean Interactions in the East Asian Marginal Seas. American Geophysical Monograph 149, pp. 299-320.

Le Bas, M.J., Le Maitre, R.W., Streckeisen, A. and Zanettin, B., 1986. A chemical classification of volcanic rocks on the total alkali-silica diagram. Journal of Petrology, 27(3): 745-750.

Lee, M.-Y. et al., 2004. First Toba supereruption revival. Limited global change due to the largest known Quaternary eruption, Toba nearly equal 74 kyr BP? Geology 32, 61-64.

Lokier, S.W., 2000. The Miocene Wonosari Formation, Java, Indonesia, Unpublished PhD Thesis, University of London..

Lourens, L.J., Hilgen, F.J., Laskar, J., Shackleton, N.J. and Wilson, D., 2004. The Neogene Period, in Gradstein, F.M., Ogg J. and Smith, A.G. (Eds), A Geological Time Scale 2004, Cambridge, pp. 409-440.

Louys, J., 2007. Limited effect of the Quaternary's largest super-eruption (Toba) on land mammals from Southeast Asia. Quaternary Science Reviews 26, 3108-3117.

Ludwig, K.R., 1980. Calculation of uncertainties of U-Pb isotope Data. Earth and Planetary Science Letters 46, 212-220.

Ludwig, K.R., 1993. Pbdat: a computer program for processing Pb-U-Th isotope data. United States Geological Survey, Open file reports, 88-542: 1-34.

Ludwig, K.R., 2003. Isoplot 3.00: A geochronological toolkit for Microsoft Excel. Berkeley Geochronology Centre Special Publication 4.

Mason, B.G., Pyle, D.M. and Oppenheimer, C., 2004. The size and frequency of the

largest explosive eruptions on Earth. Bulletin of Volcanology 66, 735-748.

Mattinson, J.M., 2005. Zircon U-Pb chemical abrasion ("CA-TIMS") method: Combined annealing and multi-step partial dissolution analysis for improved precision and accuracy of zircon ages. Chemical Geology 220, 47-66.

McCaffrey, R., 1996. Slip partitioning at convergent plate boundaries of SE Asia, in Hall, R., and Blundell, D.J (Eds), Tectonic Evolution of SE Asia: Geological Society [London] Special Publication 106, pp. 3-18.

Miller, C.F. and Wark, D.A., 2008. Supervolcanoes and their explosive supereruptions. Elements 4, 11-16.

Mundil, R., Ludwig, K.R., Metcalfe, I. and Renne, P.R., 2004. Age and timing of the End Permian mass extinctions: U/Pb geochronology on closed-system zircons. Science 305, 1760-1763.

Noble, S., Schweiters J., Condon, D.J., Crowley, Q.G., Quaas, N., Parrish, R.R. , 2006. TIMS characterization of new generation of secondary electron multiplier. EOS Transactions, American Geophysical Union, 87.

Oppenheimer, C., 2002. Limited global change due to the largest known Quaternary eruption, Toba ~74 kyr BP? Quaternary Science Reviews 21, 1593-1609.

Oppenheimer, C., 2003. Climatic, environmental and human consequences of the largest known historic eruption: Tambora volcano (Indonesia), 1815. Progress in Physical Geography27, 230-259.

Pälike, H., Frazier, J. and Zachos, J.C., 2006. Extended orbitally forced palaeoclimatic records from the equatorial Atlantic Ceara Rise. Quaternary Science Reviews 25, 3138-3149.

Petraglia, M. et al., 2007. Middle Paleolithic assemblages from the Indian Subcontinent before and after the Toba Super-eruption. Science 317, 114-116.

Rahardjo, W., Sukandarrumid. and Rosidi, H.M.D., 1995. Geological map of the Yogyakarta Quadrangle. Geological Research and Development Centre, Indonesia, Bandung.

Rampino, M.R. and Self, S., 1992. Volcanic winter and accelerated glaciation following the Toba super-eruption. Nature359, 50-52.

Rampino, M.R. and Self, S., 1993a. Bottleneck in human evolution and the Toba eruption. Science 262, 1955.

Rampino, M.R. and Self, S., 1993b. Climate-volcanism feedback and the Toba eruption of ca. 74,000 years ago. Quaternary Research 40, 269-280.

Reid, M.R., 2008. How long does it take to supersize an eruption?. Elements 4, 23-28.

Rietmeijer, F.J.M., 1993. A model for tropical-extratropical transport of volcanic ash in the lower stratosphere. Geophysical Research Letters 20, 951-954.

Robock, A., 2000. Volcanic eruptions and climate. Reviews of Geophysics 20, 191-219.

Rose, W.I. and Chesner, C.A., 1987. Dispersal of ash in the great Toba eruption, 75 ka.

Geology 15, 913-917.

Smyth, H., 2005. Eocene to Miocene basin history and volcanic activity in East Java, Indonesia. Unpublished PhD Thesis, Royal Holloway University of London.

Smyth, H., Hall, R., Hamilton, J.P. and Kinny, P., 2005. East Java: Cenozoic basins, volcanoes and ancient basement, Indonesian Petroleum Association, Proceedings of the 30th Indonesian Petroleum Association Convention. Indonesian Petroleum Association, Jakarta, pp. 251-266.

Smyth, H.R., Hall, R. and Nichols, G.J., 2008a. Cenozoic volcanic arc history of East Java, Indonesia: The stratigraphic record of eruptions on an active continental margin, in Draut, A., Clift P.D. and Scholl, D.W. (Eds), Formation and Applications of the Sedimentary Record in Arc Collision Zones. Special Paper. Geological Society of America Boulder, pp. 199-222.

Smyth, H.R., Hall, R. and Nichols, G.J., 2008b. Significant volcanic contribution to some quartz-rich sandstones, East Java, Indonesia. Journal of Sedimentary Research 78, 335-356.

Smyth, H.R., Hamilton, P.J., Hall, R. and Kinny, P., 2007. The deep crust beneath island arcs: Inherited zircons reveal a Gondwana continental fragment beneath East Java, Indonesia. Earth and Planetary Science Letters258, 269-282.

Soeria-Atmadja, R., Maury, R.C., Bellon, H., Pringgoprawiro, H., Polve, M. and Priadi, B., 1994. Tertiary magmatic belts in Java. Journal of Southeast Asian Earth Sciences 9,

13-17.

Song, S.R., Chen, C.H., Lee, M.Y., Yang, T.F., Iizuka, Y., and Wei, K.Y., 2000. Newly discovered eastern dispersal of the youngest Toba Tuff. Marine Geology 167, 303-312.

Stacey, J.S. and Kramer, J.D., 1975. Approximation of terrestrial lead isotope evolution by a two stage model. Earth and Planetary Science Letters 26, 207-221.

Stommel, H. and Stommel, E., 1983. Volcano weather: The story of 1816, the year without a summer. Seven Seas Press, Newpoer.

Surono, T.B. and Sudarno, I., 1992. Geological Map of the Surakarta-Giritontro Quadrangle. Geological Research and Development Centre, Indonesia, Bandung.

Thornton, I., 1996. Krakatau: the destruction and reassembly of an island ecosystem. First Harvard University Press. Cambridge.

Trepte, C.R. and Hitchman, M.H., 1992. Tropical stratospheric circulation deduced from satellite aerosol data. Nature 355, 626-628.

White, A.F. and Blum, A.E., 1995. Effects of climate on chemical weathering in watersheds. Geochimica et Cosmochimica Acta. 59, 1729-1747.

Wright, J.D., Miller, K.G. and Fairbanks, R.G., 1992. Early and Middle Miocene stable isotopes: implication for deep-water circulation and climate. Paleoceanography 7, 357-389.

Zartman, R.E. and Cunningham, C.G., 1995. U-Th-Pb zircon dating of the 13.8-Ma

dacite volcanic dome at Cerro Rico de Potosí, Bolivia. Earth and Planetary Science Letters 133, 227-237.

Zeilinga de Boer, J.Z. and Sanders, D.T., 2002. Volcanoes in Human History. Princeton University Press, Princeton.

7 Figure & table captions

Figure 1. The modern plate tectonic setting of Indonesia, shown on a Digital Elevation Model from SRTM (Shuttle Radar Topography Mission, NASA). The volcanoes of the Sunda Arc (small white triangles) and the locations of the eruptions of Toba, Krakatau and Tambora are indicated (large white triangles). The star marks the approximate position of the volcanic centre which produced the Semilir eruption. The arrow indicates the current Indian-SE Asia plate motion vector (McCaffrey, 1996). Also shown are the location of ODP wells referred to in the text.

Figure 2. A. Digital elevation model from SRTM of East Java, showing the centres of Oligo-Miocene volcanism marked with open circles (Smyth et al., 2008a). The white star marks the location of the Jaten Formation sandstones. B. Structure of Java, showing the three structural provinces, Southern Mountains Arc, Kendeng Basin, and the edge of the Sunda Shelf, and the modern Sunda Arc built on top of these provinces (adapted from Smyth et al., 2008a). C. Sketch of the Eocene to Miocene profile across East Java depicting the volcanoes as an island arc. D. Summary of the major element geochemical

analysis of samples from the Southern Mountains Arc (Smyth, 2005), plotted on the TAS (Total Alkalis-Silica) diagram of Le Bas et al. (1986).

Figure 3. Distribution of the products of the Southern Mountains Arc in the Batu Agung escarpment, Yogyakarta region, East Java. A. Geological map (adapted from (Lokier, 2000; Rahardjo et al., 1995; Surono and Sudarno, 1992)) and location of dated samples. B. Composite sections of the volcanic and sedimentary rocks (black lines mark the location of the sections). C. Schematic stratigraphic column with published biostratigraphic and new U-Pb zircon ages. D-G. Field photographs. D. Semilir Formation being quarried at the site of Jhs4_SEM4. showing the character of the Semilir Formation at Jhs_SEM7. E. Semilir Formation in small quarry at Jhs4_SEM7. F. Nature of the exposure of the Nglanggran Formation, breccia beds are up to 10 m thick. G. Coarse, matrix-supported, poorly sorted angular, andesitic breccia of the Nglanggran Formation.

Figure 4. SEM-CL images of zircons analyzed in this study. Images A-E Semilir Formation (A. Jhs4SEM2. B. Jhs4SEM5 C.Jhs4SEM4, D.Jhs4SEM7 and E. Jhs4SEM1) and F Jaten sample Jhs2Pac43.

Figure 5. U-Pb data for zircon analysed by SIMS. A. $^{206}Pb/^{238}U$ plot with weighted mean age calculation for Jhs4SEM1. B. $^{206}Pb/^{238}U$ plot with weighted mean age calculation for Jhs2SEM2. C. Terra-Wasserberg diagram combining data from Jhs4SEM1 and Jhs4SEM2. D. $^{206}Pb/^{238}U$ plot with weighted mean age calculation for Jhs2PAC43. E. Terra-Wasserberg diagram for Jhs2PAC43.

Figure 6. U-Pb Concordia diagrams for zircons analysed by ID-TIMS. A. All data for Jhs4SEM4 and Jhs4SEM7 (shaded). B. Younger data for both samples. Note that the analysis with dashed ellipse is not used for age calculation (due to possible Pb-loss). C. Mean $^{206}Pb/^{238}U$ age calculation.

Figure 7. Comparison of Toba and Semilir volcanic deposits. A. Map showing the distribution of the products of the proximal deposits of Toba Tuff's (simplified from Aldiss and Ghazali, 1984) and the Semilir eruption. B. Thickness profile of the Youngest Toba Tuff erupted at 74 ka (Aldiss and Ghazali, 1984; Chesner et al., 1991; Knight et al., 1986). C. Thickness profile of the Semilir Formation.

Figure 8. The potential distribution of Semilir eruption ash based on the footprint of the 74 ka eruption of Toba (Song et al., 2000) plotted on a 20 Ma plate tectonic reconstruction of SE Asia (Hall, 2002). If the ash cloud travelled to the south or to the west material deposited on the Indian Ocean Plate would have since been subducted.

Table 1. Sample location information

Table 2. U-Pb ID-TIMS data.

Supplementary material. U-Pb SIMS data table

Figure 1.

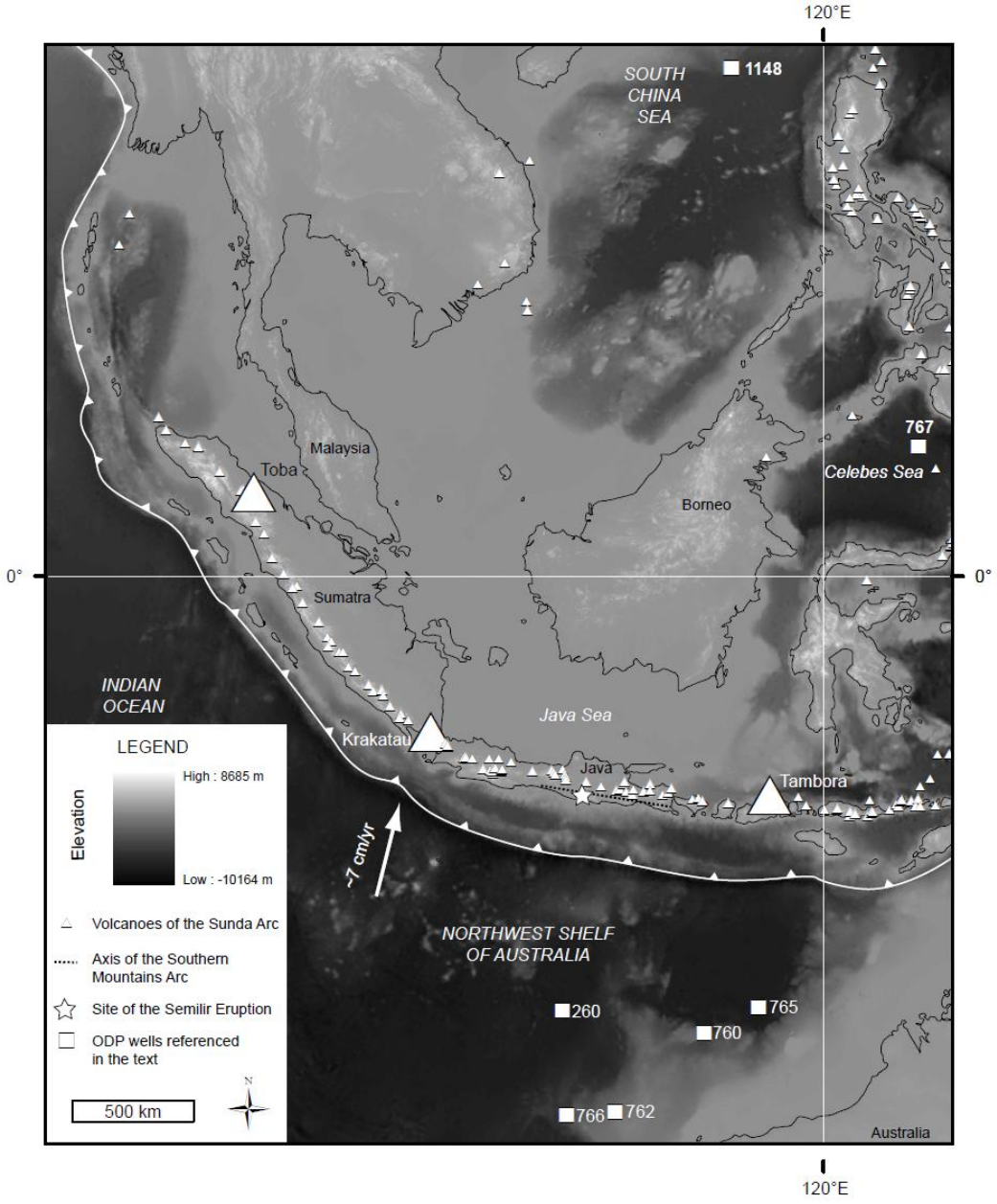

Figure 2.

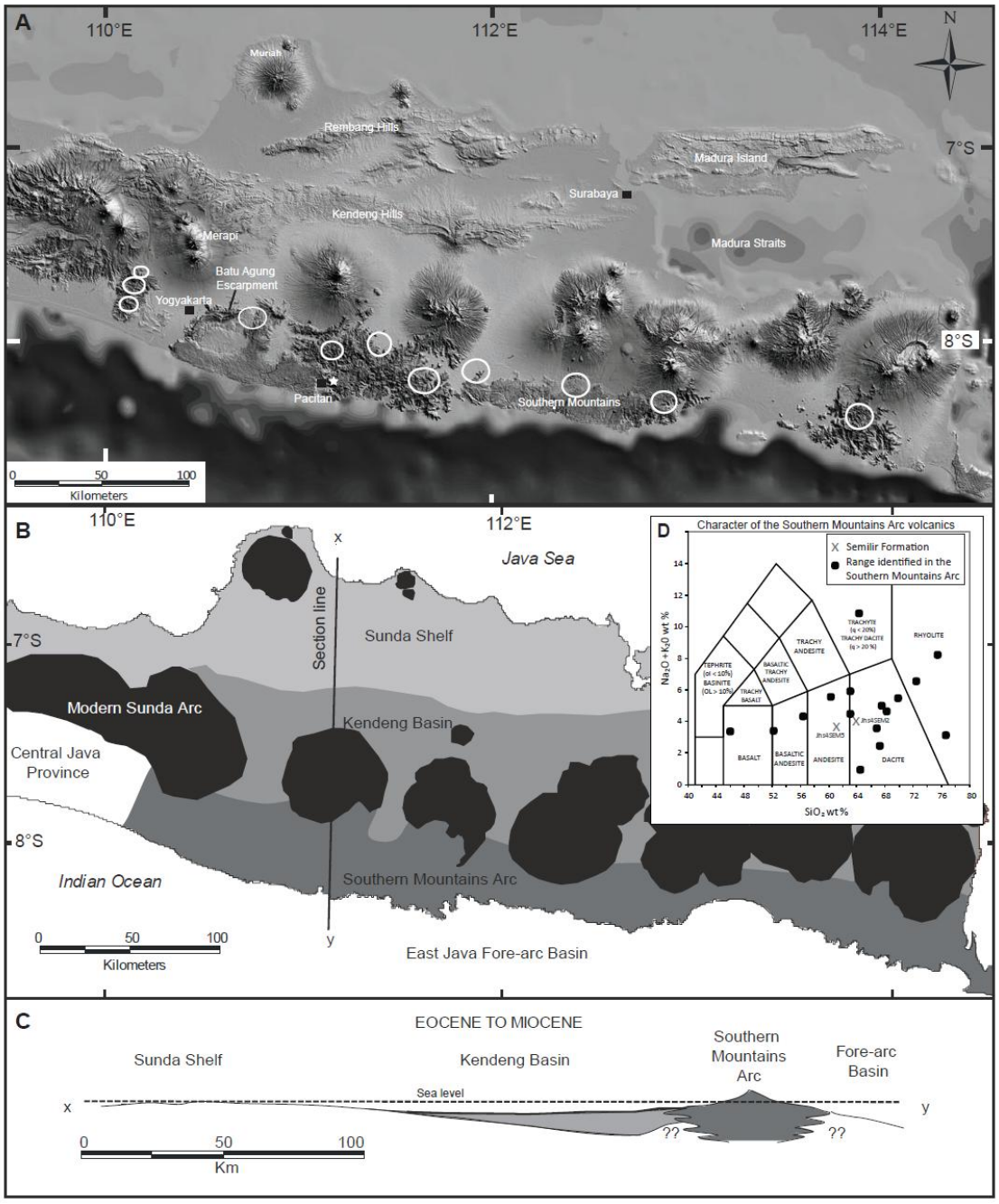

Figure 3

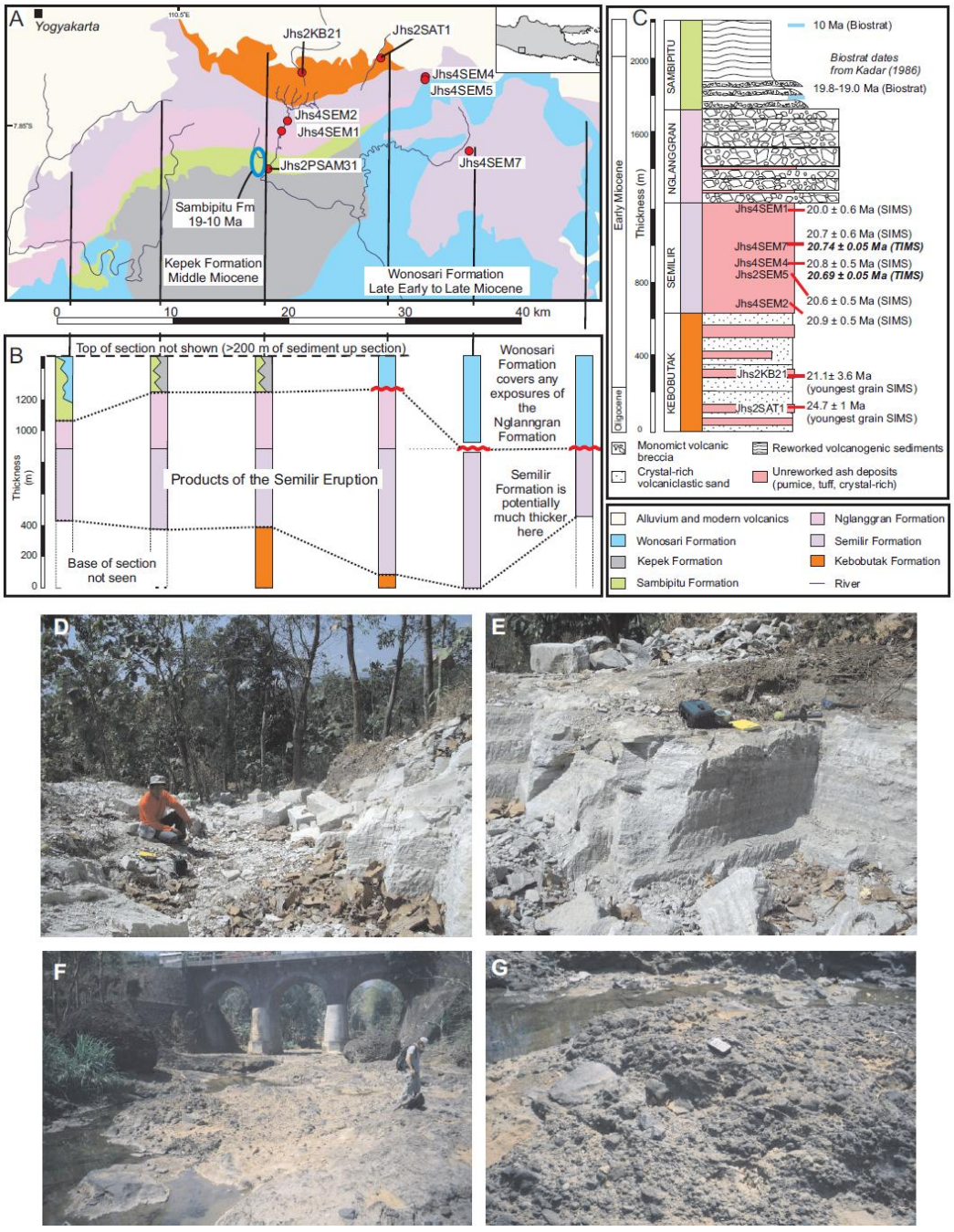

Figure 4

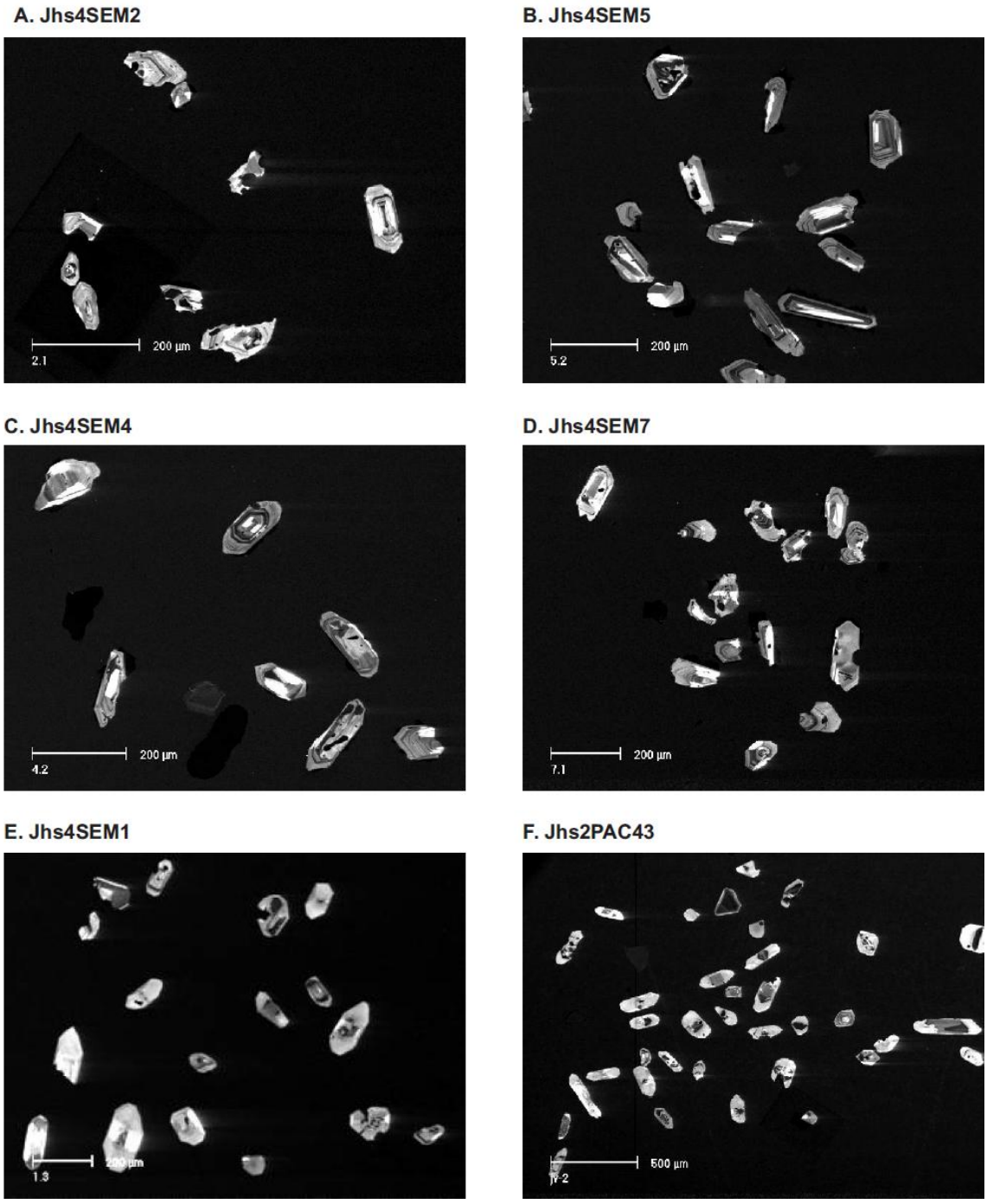

Figure 5.

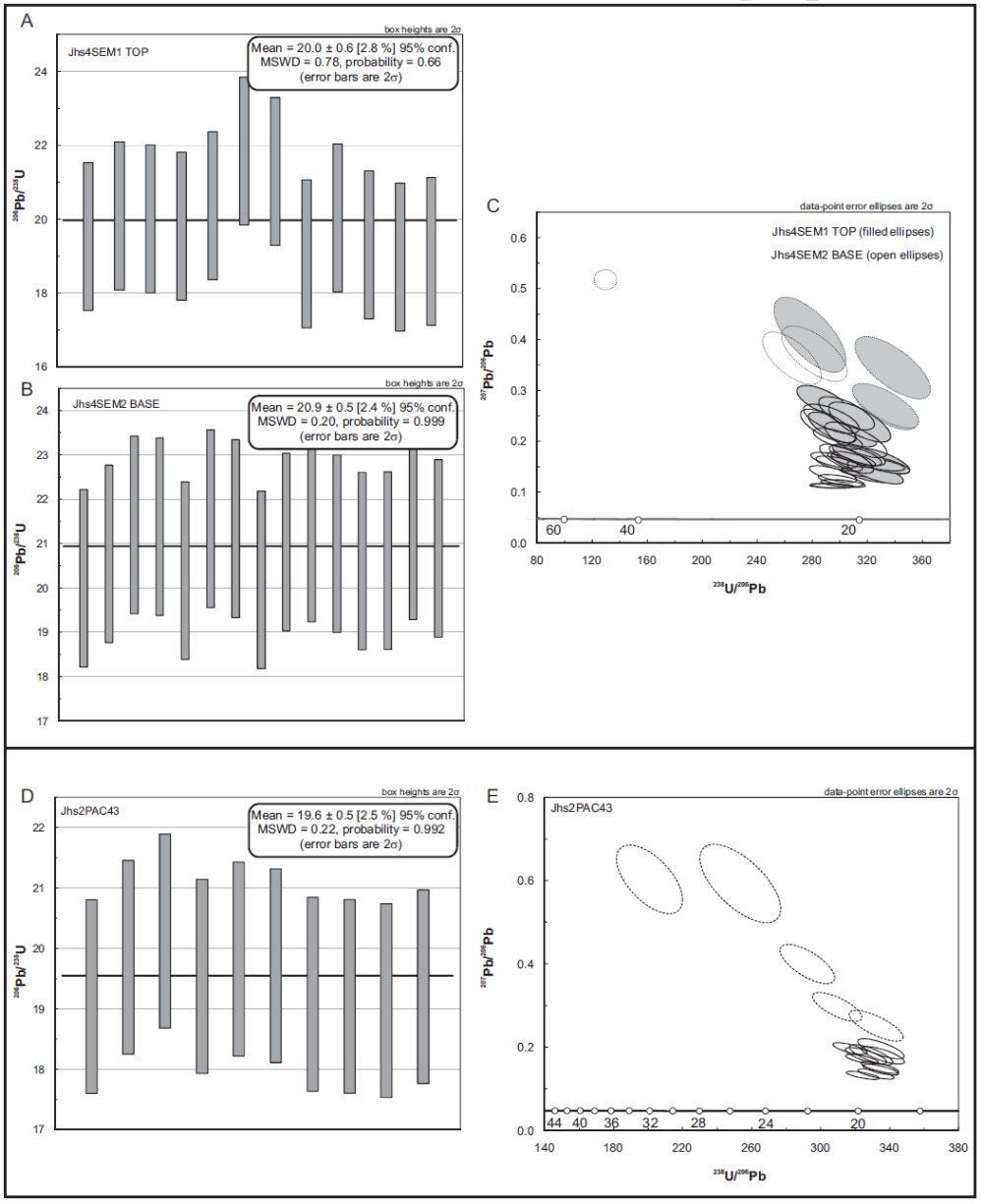

Figure 6.

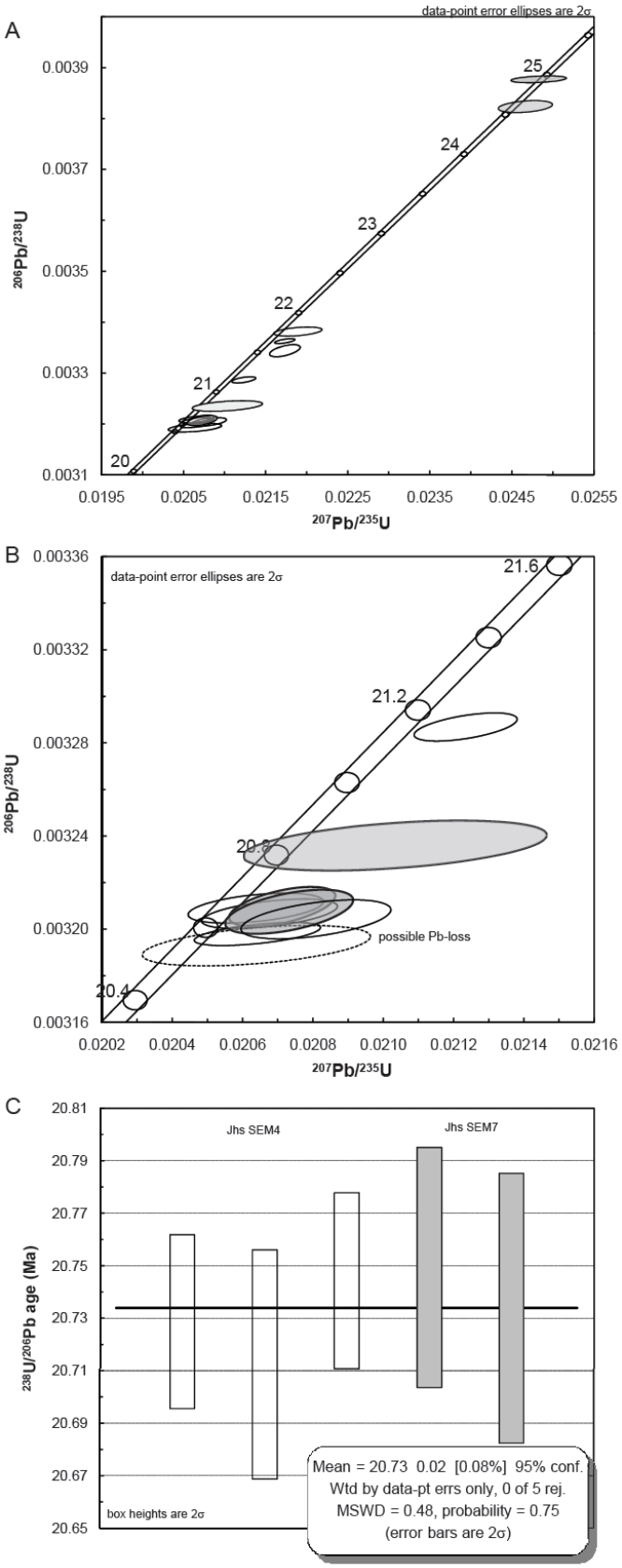

Figure 7

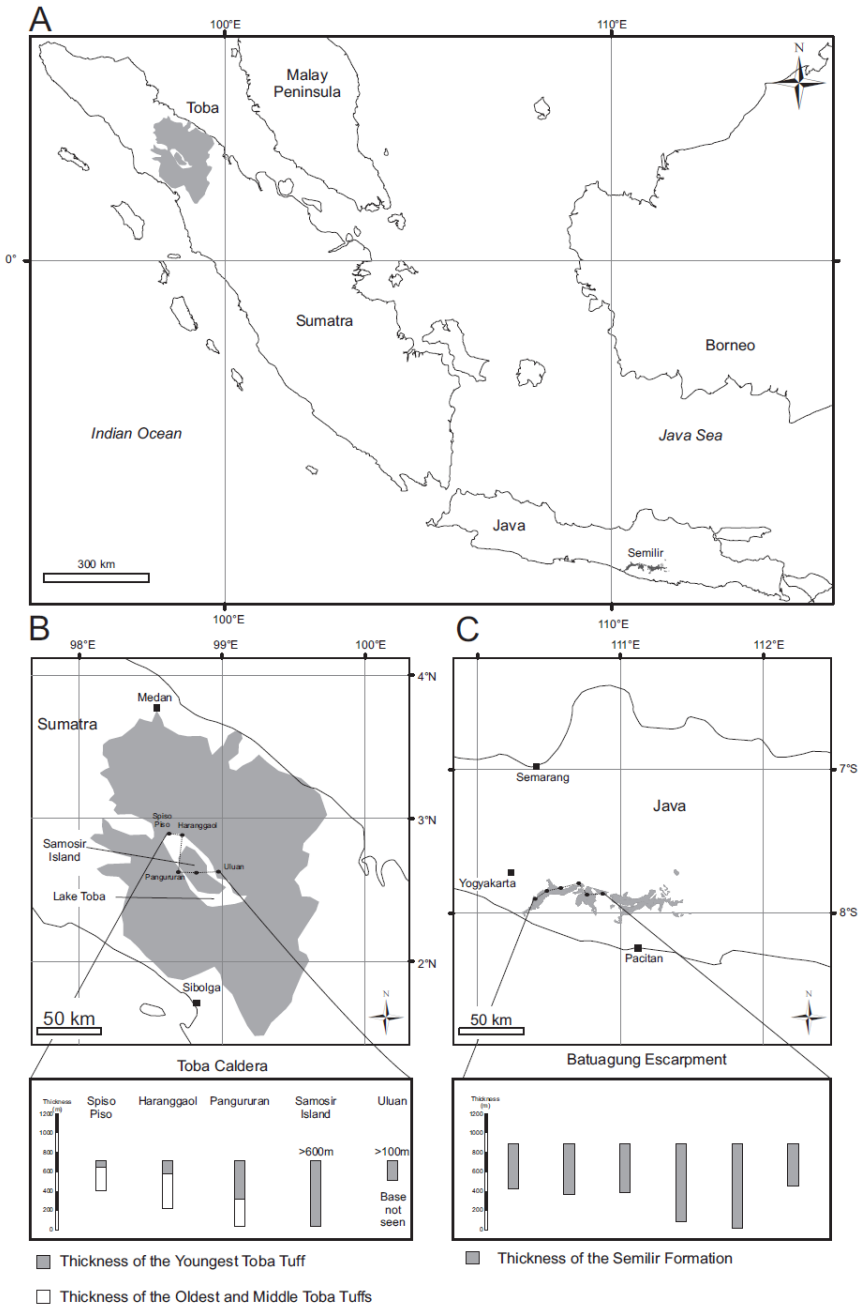

Figure 8

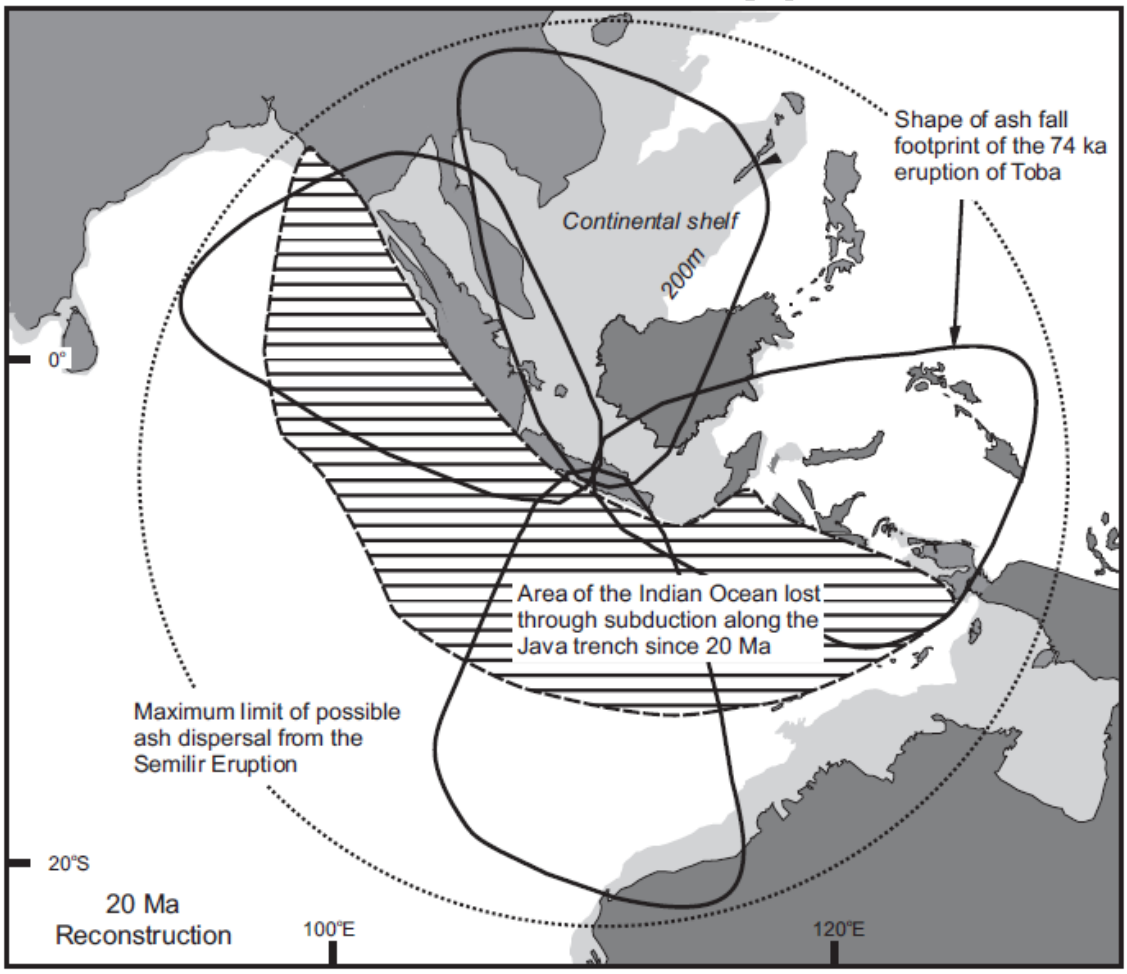

Table 1.

Formation	Sample Number	Latitude, Longitude	Lithology	Location Description
Jaten	Jhs2Pac43	8.14868S, 111.26359E	Crystal-rich sandstone, quartz- and pumice-rich	Road cut section near Tulakan, Pacitan
Semilir	Jhs4SEM1	7.85585S, 110.58601E	Thick medium grained calcareous (but not fossiliferous) ash bed.	River cliff at the top of Semilir Formation. Sample taken from the base of a 3m thick bed.
	Jhs4SEM7	7.88056S, 110.72066E	Thick non-calcareous mantling ash bed. Alternating laminations of pumice and crystals.	Small quarry cut to the south of Desa Semin. Beds are thick and gently dipping.
	Jhs4SEM4	7.81354S, 110.69958E	Massive white non-calcareous ash bed.	New road and quarry cut section very fresh exposure. Thick well bedded sequence.
	Jhs4SEM5	7.81354S, 110.69958E	Well laminated (colour banding reflecting composition), grey non-calcareous ash.	New road and quarry cut section very fresh exposure.
	Jhs4SEM2	7.84794S, 110.59071E	Pumiceous, non-calcareous, grey, rich in charcoal fragments, diffuse and well defined laminations.	On valley side small quarry cut very fresh and well exposed. Bed are more than 1m thick.
Kebobutak	Jhs2Sat1	7.78863S, 110.6665E	Volcaniclastic, granular, crystal-rich white sandstone.	Road cut near Desa Santren.
	Jhs2JKB21	7.80938S, 110.592E	Volcaniclastic grey sandstone,	Roadside exposure on the north flank of Batu Agung Escarpment.

Table 2

		Compositional Parameters								Radiogenic Isotope Ratios								Isotopic Ages					
	Wt.	U	Th	Pb	^{206}Pb*	mol %	Pb*	Pb_c	^{206}Pb	^{208}Pb	^{207}Pb		^{207}Pb		^{206}Pb		corr.	^{207}Pb		^{207}Pb		^{206}Pb	
Sample	mg	ppm	U	ppm	x10^{-13} mol	^{206}Pb*	Pb_c	(pg)	^{204}Pb	^{206}Pb	^{206}Pb	% err	^{235}U	% err	^{238}U	% err	coef.	^{206}Pb	±	^{235}U	±	^{238}U	±
(a)	(b)	(c)	(d)	(c)	(e)	(e)	(e)	(e)	(f)	(g)	(g)	(h)	(g)	(h)	(g)	(h)		(i)	(h)	(i)	(h)	(i)	(h)
Jhs SEM4																							
Z1	0.010	404	0.740	1.6	0.5183	95.63%	7	1.93	426	0.239	0.046766	0.696	0.020677	0.763	0.003207	0.161	0.504	26.80	16.65	20.78	0.16	20.73	0.03
Z2	0.056	85	0.781	0.4	0.6342	95.08%	6	2.68	377	0.254	0.047099	0.756	0.020808	0.839	0.003204	0.212	0.497	43.92	18.03	20.91	0.17	20.71	0.04
Z3	0.020	211	0.870	0.9	0.5673	95.32%	7	2.28	397	0.281	0.046815	0.649	0.020642	0.711	0.003198	0.127	0.551	29.63	15.54	20.75	0.15	20.67	0.03
Z4	0.020	145	0.863	0.7	0.3930	91.70%	4	2.91	224	0.280	0.046881	1.200	0.020639	1.285	0.003193	0.222	0.456	32.99	28.69	20.74	0.26	20.64	0.05
Z5	0.032	83	0.747	0.3	0.3497	94.47%	6	1.66	336	0.241	0.046642	0.707	0.020637	0.762	0.003209	0.163	0.434	20.45	16.94	20.74	0.16	20.74	0.03
Z6	0.023	273	0.745	1.1	0.8825	97.66%	14	1.72	794	0.242	0.047136	0.587	0.021734	0.699	0.003344	0.291	0.563	46.13	13.99	21.83	0.15	21.61	0.06

Z7	0.029	181	0.803	0.8	0.7256	95.94%	8	2.51	458	0.260	0.046869	0.403	0.021733	0.465	0.003363	0.115	0.624	32.72	9.64	21.83	0.10	21.73	0.02
Z8	0.040	188	0.865	0.8	1.0222	97.39%	13	2.23	713	0.280	0.046856	0.496	0.021234	0.564	0.003287	0.150	0.559	31.99	11.87	21.34	0.12	21.24	0.03
Jhs SEM7																							
Z1	0.006	597	0.758	2.4	0.4959	95.51%	7	1.90	414	0.245	0.046804	0.520	0.020714	0.605	0.003210	0.222	0.538	28.80	12.45	20.82	0.12	20.75	0.05
Z2	0.026	139	0.641	0.7	0.5920	96.08%	8	1.93	476	0.205	0.046456	1.070	0.024840	1.112	0.003878	0.144	0.349	12.24	25.70	24.91	0.27	25.05	0.04
Z3	0.021	165	0.782	0.8	0.5623	95.51%	7	2.12	416	0.252	0.046794	1.048	0.024677	1.106	0.003825	0.257	0.334	29.82	25.09	24.75	0.27	24.70	0.06
Z4	0.024	85	0.622	0.4	0.2941	94.27%	5	1.45	325	0.202	0.046957	1.035	0.021901	1.108	0.003383	0.215	0.428	36.81	24.72	22.00	0.24	21.86	0.05
Z5	0.026	158	0.828	0.7	0.5387	95.66%	7	1.99	428	0.268	0.046879	0.632	0.020734	0.724	0.003208	0.249	0.519	32.81	15.10	20.84	0.15	20.73	0.05
Z6	0.023	77	0.729	0.4	0.2418	91.03%	3	0.15	207	0.237	0.047143	1.576	0.021035	1.672	0.003236	0.265	0.429	46.07	37.59	21.14	0.35	20.92	0.06

(a) z1, z2 etc. are labels for fractions composed of zircon grains or fragments; all fractions annealed and chemically abraded after Mattinson (2005).

(b) Nominal fraction weights estimated from photomicrographic grain dimensions, adjusted for partial dissolution during chemical abrasion.

(c) Nominal U and total Pb concentrations subject to uncertainty in photomicrographic estimation of weight and partial dissolution during chemical abrasion.

(d) Model Th/U ratio calculated from radiogenic 208Pb/206Pb ratio and 207Pb/235U age.

(e) Pb* and Pbc represent radiogenic and common Pb, respectively; mol % ^{206}Pb* with respect to radiogenic, blank and initial common Pb.

(f) Measured ratio corrected for spike and fractionation only. SEM analyses, based on analysis of NBS-981 and NBS-982.

(g) Corrected for fractionation, spike, and common Pb; up to 1 pg of common Pb was assumed to be procedural blank:
206Pb/204Pb = 18.70 ± 0.80%; 207Pb/204Pb = 15.56 ± 0.32%;

208Pb/204Pb = 36.82 ± 0.74% (all uncertainties 1-sigma). Excess over blank was assigned to initial common Pb 206Pb/204Pb = 18.55 ± 0.80%; 207Pb/204Pb = 15.62 ± 0.32%;

208Pb/204Pb = 38.45 ± 0.74%.

(h) Errors are 2-sigma, propagated using the algorithms of Schmitz and Schoene (2007) and Crowley et al. (2007).

(i) Calculations are based on the decay constants of Jaffey et al. (1971). 206Pb/238U and 207Pb/206Pb ages corrected for initial disequilibrium in 230Th/238U using Th/U [magma] = 4.5.

(j) Corrected for fractionation, spike, and blank Pb only.

Highlights

- We report an Early Miocene major eruption in Java, Indonesia, the Semilir Event
- The event occurred over a narrow time interval peaking at 20.72 ± 0.02 Ma
- First pre-Pleistocene record of a major volcanic eruption in SE Asia
- An event such as Semilir Eruption could certainly have triggered a climate response